FITTING OF THE PARAMETERS OF STIFFNESS AND DAMPING TO FLEXIBLE COUPLING MODELS IN ROTOR-BEARING-COUPLING SYSTEMS BY USING FREQUENCY RESPONSE FUNCTIONS

Abdón Tapia Tadeo
Katia Lucchesi Cavalca
UNICAMP - Universidade Estadual de Campinas, Departamento de Projeto Mecânico
Postal Box: 6051-13083-970, Campinas - SP - Brasil
Phone: (021)-(055)-(19)-37883166, Fax: (021)-(055)-(19)-32893722
E-mail: **abdon@fem.unicamp.br**
E-mail: **katia@fem.unicamp.br**

Abstract. Most model fitting techniques for mechanical systems modelled by finite elements require the identification of experimental modal parameters, which are obtained through modal tests. But, in the case of real rotating rotor-coupling-bearing systems, the accomplishment of complete modal tests is frequently not possible, due to the difficulties present in the excitation process of the rotating components of the system, either by using electric exciters (shaker) or impact exciters (hammer). In this article, the possibility of fitting the finite element model of a rotor-coupling-bearing system is introduced. The process consists in the evaluation of stiffness and damping coefficients of the coupling by using the frequency response function (FRF) due to residual unbalance (inherent condition of operation for rotating systems), or due to an external aleatory excitation. The fitting procedure consists in applying an iterative non-linear method for parameters fitting to determine the unknown coefficients of the model, which values are initially assumed. The estimate problem is a non-linear problem of minimum squares, where the objective function to be minimized is the sum of the square of the difference among magnitudes of the theoretical and experimental frequency response functions. The finite element model of the system only considers the transversal vibrations. The well-known linear models are considered for rotors, bearings and rigid disks. In the same way, the flexible coupling of the system is modelled using simplified linear models recommended in the literature.

Key words: flexible couplings, flexible rotors, bending vibrations, finite elements, and rotordynamics.

1. Introduction

In the mechanical systems, unbalance and misalignment of the shafts represent two important sources of vibrations. Otherwise, the lack of information about forces and moments generated in the axial coupling between shafts due to misalignment makes difficult the clear understanding of the influence of this component in the system. It is not possible to consider a unique simplified mathematical finite element model for these joining elements. Tapia A. and Cavalca K. (2001) implemented, based on the models of Nelson H. and Crandall S. (1992) and Kramer E. (1993), five simplified models to represent the mechanical couplings in transversal vibrations analysis of rotor-coupling-bearing power transmission systems. The couplings were considered through a mass-spring-damper system. Xu et al (1994) analyzed the vibrations of a flexible rotor-motor-coupling system using the component mode synthesis technique, in which the coupling is described through several nodes. In this sense, the present work search to adjust the theoretical models of the rotor-coupling-bearing systems, considering each one of the 5 models introduced by Tapia A. and Cavalca K. (2001), using the frequency response curves (*FRFs*) of the system for the fitting process. The fitting procedure uses the Non-Linear Minimum Squares Method based on the previous work of Arruda J.R.F. and Duarte M.V. (1987, 1989).

2. The Rotor-Coupling-Bearing Mechanical System.

Fig. (1) shows the inertial and auxiliary reference systems considered for Rotor-Coupling-Bearing Systems. In this work, only the bending vibrations of the system are considered. An inertial reference system *XYZ* and an auxiliary reference system *xyz*, fixed in the shaft, describe the equations of motion of the system. A generic cross section of the bending rotor is defined regarding the system *XYZ* through the generalized coordinates (u,v,α,β). $u(Y,t)$, $v(Y,t)$ are the translations in *X* and *Z* directions, which supply the cross section centre position at the instant *t*. $\alpha(Y,t)$ and $\beta(Y,t)$ supply the orientation of the cross section around *X* and *Z* axes respectively.
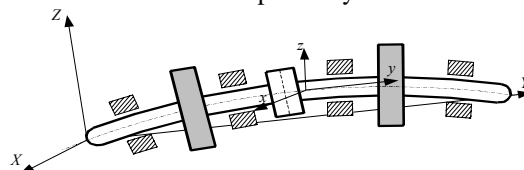

Figure 1. Reference Systems for Rotor-Coupling-Bearing System.

1

The finite element models used to represent flexible shafts, rigid disks and bearings are described in Tapia A. and Cavalca K. (2001). The shafts are modelled by flexible beam elements of continuous mass; the disks are modelled as rigid components with concentrated masses; the bearings are represented by stiffness and damping equivalent coefficients, neglecting bending moments and oil film inertia effects in these components.

3. Mechanical Couplings

According to Tapia A. (2003), there are few simplified models to represent mechanical couplings in Rotor-Coupling-Bearing Systems. Therefore, there is less discussion about what simplified model can be the best representation for the physical problem involving the mechanical axial coupling (rigid or flexible). In Tapia A. (2003) the following models were implemented.

3.1. Kramer Models

The first model considered to represent the flexible couplings in the modelling of rotating systems takes into account the considerations given by Kramer E. (1993), according to Fig. (2a). This model consists of two free-free shafts with 8 degrees of freedom each one. The coupling effect consists in constraining the translation degrees of freedom before node i and after node j of the coupling. In this case, the displacements are equal in x and y directions, $u_i=u_j$ and $v_i=v_j$. The system, initially with 16 degrees of freedom, is reduced to a system with 14 degrees of freedom, due to the coupling effect, as shown in Fig. (2b). This coupling model was applied by Sekhar et al. (1996).
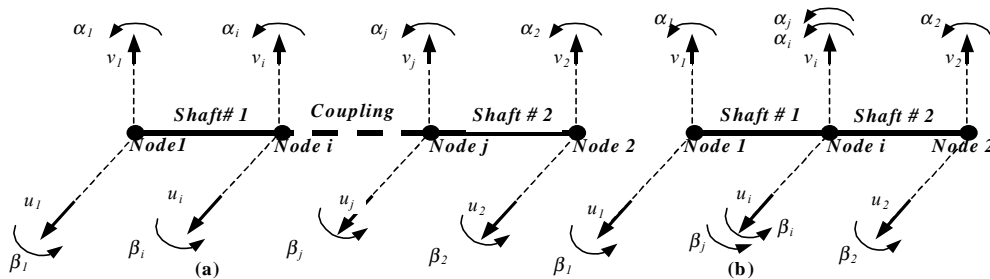

Figure 2. (a) Mechanical System of two shafts axially coupled, (b) The 1st Kramer model for couplings.

The second model studied, according to Kramer E. (1993), takes into account the stiffness k_R and the damping c_R of the coupling. In this case, the same constrains of the 1st model are maintained, according to Fig. (3).
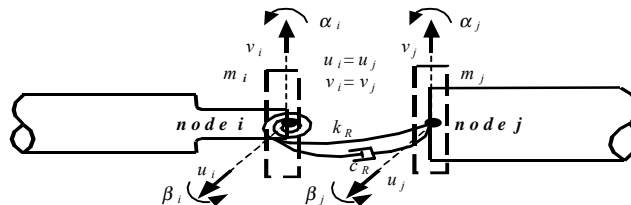

Figure 3. The 2nd Kramer model for flexible couplings.

3.2. Nelson and Crandall Models

The third model takes into account the considerations stated by Nelson H. and Crandall S. (1992). This model represents the coupling as an elastic component with isotropic translational stiffness k_T and rotational stiffness k_R, between the stations i and j, corresponding to the connecting points of the shafts, as shown in Fig. (4a). The fourth model is also according to the considerations stated by Nelson H. and Crandall S. (1992). This model considers stiffness and damping of the coupling, through both translational and rotational equivalent stiffness and damping coefficients (k_T, k_R, c_T, c_R) according to Fig. (4b).
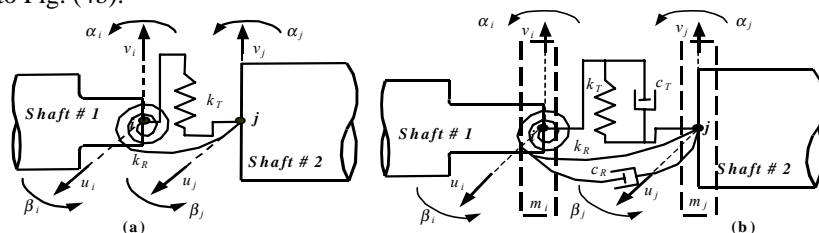

Figure 4. Nelson and Crandall Models: (a) 3rd Model; (b) 4th Model.

In the four models presented, the inertia effects are included considering two rigid disks located in both stations of the shafts connection. The 5th model considered in the analysis is the rigid disk model (or rigid coupling). The equation of motion of the coupling, for each model previously described is written in the following form:

$$[M_a]\begin{Bmatrix} \{\ddot{q}_i\} \\ \{\ddot{q}_j\} \end{Bmatrix} + [\Omega[G_a] + [C_a]]\begin{Bmatrix} \{\dot{q}_i\} \\ \{\dot{q}_j\} \end{Bmatrix} + [K_a]\begin{Bmatrix} \{q_i\} \\ \{q_j\} \end{Bmatrix} = \{F_{ex}\} + \{F_{con}\}.$$ (1)

Where:

$\{F_{con}\}$, $\{F_{ex}\}$ are the connecting forces and external forces vectors, acting on the coupling;

$[M_a]$, $[G_a]$ are the mass and gyroscopic matrices due to the coupling;

$[C_a]$, $[K_a]$ are the damping and stiffness matrices due to the coupling. The damping matrix can be null depending on the model (Tapia A. 2003).

These physical coupling models are isotropic models of mass-spring-damper systems, in which low values of translational and/or rotational stiffness coefficients approach the dynamical behaviour of flexible couplings, as well high values of the same parameters simulate approximately rigid coupling.

4. Equation of Motion for Rotor-Coupling-Bearing Systems

After the equations of motion were defined for each component of the system, the complete equation of motion for the whole system (Eq. (2)) can be obtained by the Direct Stiffness Method (DSM) described by Nelson H. and Crandall S. (1992).

$$[M_g]\{\ddot{q}_g\} + [\Omega[G_g] + [C_g]]\{\dot{q}_g\} + [K_g]\{q_g\} = \{F_{ex}\}.$$ (2)

Where: $[M_g]$ is the global mass matrix of the system, generally symmetric, and containing the concentrated masses of rigid disks and coupling, as well as the masses of beam elements of the shaft; $[G_g]$ is the global gyroscopic matrix of the system, containing the contribution of the previous components, although this matrix is non-symmetric and it depends on the rotational speed of the rotor Ω; $[C_g]$ and $[K_g]$ are the global dissipative (damping) and stiffness matrices of the system, containing the flexible shaft elements, bearings and coupling contributions; $\{F_{ex}\}$ is the external forces vector; $\{\ddot{q}_g\}$, $\{\dot{q}_g\}$, $\{q_g\}$ are the global acceleration, velocity and displacement vectors of the system in principal co-ordinates.

5. Frequency Response Functions of the System

Two types of frequency response functions *FRFs* are considered in the analysis: the residual unbalance response of the system *FRD* and the transfer function due to an aleatory excitation force *FRF*.

5.1. Unbalance Response Function (*FRDs*)

The external forces due to a residual unbalance $\{F_d\}$ and the system response $\{q_d\}$ to this excitation force can be written in the following form:

$$\{F_d\} = \{F_c\}Cos(\Omega t) + \{F_s\}Sin(\Omega t) \; ; \; \{q_d\} = \{q_c\}Cos(\Omega t) + \{q_s\}Sin(\Omega t).$$ (3)

Substituting $\{F_d\}$ and $\{q_d\}$ in Eq. (2) for known coefficients of the vectors $\{F_c\}$ and $\{F_s\}$ of the unbalance external force ($\{F_d\}=\{F_{ex}\}$), the coefficients of the vectors $\{q_c\}$ and $\{q_s\}$ can be determined:

$$\begin{Bmatrix} \{q_c\} \\ \{q_s\} \end{Bmatrix} = \begin{bmatrix} [K_g] - \Omega^2[M_g] & \Omega[\Omega[G_g] + [C_g]] \\ -\Omega[\Omega[G_g] + [C_g]] & [K_g] - \Omega^2[M_g] \end{bmatrix}^{-1} \begin{Bmatrix} \{F_c\} \\ \{F_s\} \end{Bmatrix}.$$ (4)

Substituting these coefficients in the equation that describes $\{q_d\}$, the unbalance response of the system can be obtained in the time domain. Otherwise, the unbalance response function *(FRD)* of the system can be obtained by combining the same coefficients.

5.2. Transfer Function in the Frequency Domain

The transfer function in the frequency domain is also named frequency response function (FRF). The FRF is defined by considering a sinusoidal excitation through a group of forces with the same frequency ω, but with different amplitudes and phases, represented by $\{F_{ex}\}=\{F_o\}e^{i\omega t}$. The system response can be defined as $\{q_g\}=\{q_o\}e^{i\omega t}$. The equation of motion of the system becomes:

$$\left[-\omega^2[M_g]+i\omega[\Omega[G_g]+[C_g]]+[K_g]\right]\{q_o\}=\{F_o\}. \tag{5}$$

Finally, the transfer functions matrix $[H(\omega)]$ is given by:

$$[H(\omega)]=\left[-\omega^2[M_g]+i\omega[\Omega[G_g]+[C_g]]+[K_g]\right]^{-1}. \tag{6}$$

Therefore, any of the transfer functions $H_{jk}(\omega)$ can be defined by the modal superposition method given bellow:

$$H_{jk}(\omega)=\frac{q_{oj}}{F_k}=\sum_{r=1}^{2n}\frac{q_{odjr}\cdot q_{oekr}}{i\omega b_r+a_r}\ ,\quad with:\ q_{odjr}\in\{q_{od}\}_r\ ,\ q_{oekr}\in\{q_{oe}\}_r. \tag{7}$$

Where:

$H_{jk}(\omega)$ is the transfer function for the *j-th* d.o.f. (q_{oj}) due to a force (F_k) acting on the *k-th* d.o.f., at a frequency ω;

$\{q_{od}\}_r$ is the right eigenvector corresponding to the eigenvalue λ_r and q_{odjr} is the *j-th* component;

$\{q_{oe}\}_r$ is the left eigenvector corresponding to the eigenvalue λ_r and q_{oekr} is the *k-th* component;

a_r , b_r are diagonal terms of the matrices ($[diag(a_r)]$, $[diag(b_r)]$), defined by the orthogonality property of the modal matrices of the right modes $[Xd]$ and left modes $[Xe]$ of the system, as given bellow:

$$[Xe]^t[B][Xd]=[diag(b_r)],\ [Xe]^t[A][Xd]=[diag(a_r)],\ \text{with:}\ [A]=\begin{bmatrix}-[M_g] & [O]\\ [O] & [K_g]\end{bmatrix},[B]=\begin{bmatrix}[O] & [M_g]\\ [M_g] & \Omega[G_g]+[C_g]\end{bmatrix}.$$

6. Sensitivity Matrix of the Frequency Response Functions

Duarte M.A.V. (1994) defined sensitivity of frequency response functions by using the first order finite differences, applying the partial derivatives of the *FRFs* related to the structural parameters of the rotor. (Tapia A. 2003) gives the FRF matrix for a rotating system, using the mechanical impedance matrix:

$$[H(\omega)]=\left[-\omega^2[M_g]+i\omega[\Omega[G_g]+[C_g]+[CV_g]]+[K_g]\right]^{-1}. \tag{8}$$

Where: ω is the frequency of the excitation force; $[M_g]$, $[C_g]$, $[K_g]$, $[G_g]$ are the global matrices of mass, damping, stiffness, and gyroscopic matrix of the system; $[CV_g]$ is the proportional viscous damping matrix of the system.

The sensitivity of any *FRF* related to a parameter p_k, using the derivative property of the inverse matrix, is defined by:

$$\frac{\partial[H(\omega)]}{\partial p_k}=-[[IM]^{-1}]^t\frac{\partial[IM]}{\partial p_k}[IM]^{-1},\ \text{with:}\ [IM(\omega)]=-\omega^2[M_g]+i\omega[\Omega[G_g]+[C_g]+[CV_g]]+[K_g]. \tag{9}$$

Where: $\dfrac{\partial[IM(\omega)]}{\partial p_k}=-\omega^2\dfrac{\partial[M_g]}{\partial p_k}+i\omega\left[\Omega\dfrac{\partial[G_g]}{\partial p_k}+\dfrac{\partial[C_g]}{\partial p_k}+\dfrac{\partial[CV_g]}{\partial p_k}\right]+\dfrac{\partial[K_g]}{\partial p_k}.$

For a FRF $H_{ij}(\omega)$, an element of the sensitivity matrix $[S]_{ptxnp}$ is defined by:

$$S_{lk}=\frac{\partial H_{ij}(\omega_l)}{\partial p_k};\quad with:\ l=1,..,pt\ ;k=1,..,pn\ \ (pt:\text{number of points of } FRF;\text{np}:\text{number of parameters})\cdot \tag{10}$$

The derivatives present in Eq. (10) can be obtained analytical or numerically, which means a certain difficulty level, depending on the complexity of the system modelled. Therefore, the sensitivity matrix is defined by finite differences, applying the Brown and Dennis rules (Duarte M. 1981), as follow:

$$S_{lk}(\omega_l)=\frac{H_{ij}(\omega_l)\big|_{p_k+\Delta p_k}-H_{ij}(\omega_l)\big|_{p_k}}{\Delta p_k};\ \Delta p_k=\begin{cases}10^{-9} & \text{se}\ |p_k|<10^{-6}\\ 10^{-3}|p_k| & \text{se}\ |p_k|\ge10^{-6}\end{cases}\ \text{with:}\ l=1,...,npt\ ;k=1,...,np\cdot \tag{11}$$

7. Models Fitting

In the present work the model fitting of the rotor-coupling-bearing systems applies the variation of the model parameters to the coupling. The process uses the Non-linear Minimum Square Algorithm based on the previous work of Arruda, J.R.F. (1987,1989). The algorithm was adapted to the fitting process in the frequency domain, which can be an unbalance response *FRD*, or a transfer function due to an aleatory excitation *FRF*. These curves are nominated

frequency response functions (*FRFs*) and they are applied to adjust the coupling parameters in the rotor-coupling-bearing system. The experimental *FRFs* measured at the nodes (*1...nos*) are named *FRF*$_{exp}$, and the *FRFs* obtained through the theoretical model are named *FRF*. The vector of the estimated parameters is $\{p\}_{npx1}$ where *np* is the number of parameters to be evaluated. The objective function (*F*$_{obj}$) is the sum of the squares of the difference between the experimental measurements and the simulated responses:

$$F_{obj} = \left\{\{FRF_{exp}\}_{ptx1} - \{FRF\}_{ptx1}\right\}^t [W]\left\{\{FRF_{exp}\}_{ptx1} - \{FRF\}_{ptx1}\right\}, \text{ where} \tag{12}$$

$$\{FRF\}_{ptx1} = \{f_1(\omega_1),..., f_1(\omega_n),..., f_{nos}(\omega_1),..., f_{nos}(\omega_n)\}^t, \{FRF_{exp}\}_{ptx1} = \{fe_1(\omega_1),..., fe_1(\omega_n),..., fe_{nos}(\omega_1),..., fe_{nos}(\omega_n)\}^t.$$

Where: *pt* is the total number of points considering all *FRFs*; [*W*]$_{ptxpt}$ is the positive definite weighted matrix with dimension *ptxpt*; $fe_i(\omega_i), f_i(\omega_i)$ are the experimental and simulated frequency response functions, respectively in node *i* and at the frequency ω_i; *n* is the number of points for each *FRF*.

Defining a generic coefficient S_{ij} of the sensitivity matrix [*S*] as $S_{ij} = \partial f(\omega_i)/\partial p_j$, the complete sensitivity matrix is obtained:

$$[S] = \left[\frac{\partial\{FRF\}_{ptx1}}{\partial\{p\}_{npx1}}\right] = \begin{bmatrix} \partial f_1(\omega_1)/\partial p_1 & \partial f_1(\omega_1)/\partial p_2 & ... & \partial f_1(\omega_1)/\partial p_{np} \\ ::::: & ::::: & ::::: & ::::: \\ \partial f_1(\omega_n)/\partial p_1 & \partial f_1(\omega_n)/\partial p_2 & ... & \partial f_1(\omega_n)/\partial p_{np} \\ ::::: & ::::: & ::::: & ::::: \\ \partial f_{nos}(\omega_1)/\partial p_1 & \partial f_{nos}(\omega_1)/\partial p_2 & ... & \partial f_{nos}(\omega_1)/\partial p_{np} \\ ::::: & ::::: & ::::: & ::::: \\ \partial f_{nos}(\omega_n)/\partial p_1 & \partial f_{nos}(\omega_n)/\partial p_2 & ... & \partial f_{nos}(\omega_n)/\partial p_{np} \end{bmatrix}_{ptxnp}. \tag{13}$$

Each sensitivity coefficient is evaluated by Eq. (11). The algorithm that evaluates the parameter by Non-linear Minimum Square consists of the following steps:
- To calculate the Jacobian (sensitivity matrix), of the vector $\{FRF\}_{ptx1}$, until the parameters to be estimated $\{p\}_{npx1}$ assume the value corresponding to the *k*-th iteration $\{p\}^k$. The Jacobian is given by:

$$[S]^k = \left[\frac{\partial\{FRF\}_{ptx1}}{\partial\{p\}_{npx1}}\right]_{\{p\}=\{p\}^k}. \tag{14}$$

- To determine the search direction of the optimal vector $\{p\}_{npx1}$ for the next iteration, using the minimum concept for the objective function:

$$\nabla(F_{obj})\big|_{\{p\}=\{p\}^k} = \begin{Bmatrix} \partial F_{obj}/\partial p_1 \\ \vdots \\ \vdots \\ \partial F_{obj}/\partial p_{np} \end{Bmatrix}_{\{p\}=\{p\}^k} = \begin{Bmatrix} 0 \\ \vdots \\ \vdots \\ 0 \end{Bmatrix}.$$

Applying this condition to the objective function, Eq. (15) can be written:

$$[W]^k.[S]_k^t.\{\Delta p\}^k = [W]^k.\left\{\{FRF_{exp}\} - \{FRF\}^k\right\}. \tag{15}$$

Generally in Eq. (15) $pt > np$, so that the solution uses the generalised inverse definition or pseudo-inverse ([ ]$^+$). The search direction $\{\Delta p\}^k$ is obtained as:

$$\{\Delta p\}^k = \left[[W]^k.[S]_k^t\right]^+.[W]^k.\left\{\{FRF_{exp}\} - \{FRF\}^k\right\}. \tag{16}$$

- To calculate the next vector of estimated parameters $\{p\}^{k+1}$, which is function of $\{p\}^k$ and $\{\Delta p\}^k$:

$$\{p\}^{k+1} = \{p\}^k + \alpha\{\Delta p\}^k. \tag{17}$$

In Eq. (17) the value of α must be determined through a unidimensional search method along a straight line. The Coggin Method was applied in this case, which avoid the derivative functions. The successful linear search must satisfy the condition $F_{obj}^{k+1} < F_{obj}^{k}$.

- If the linear search is not successful, the sensitivity matrix $[S]^k$ is modified for the k-th iteration, introducing a damping factor λ, and rewriting the sensitivity matrix:

$$[S]^k = [S]^k + \lambda [Q]^k .$$ (18)

Where $[Q]^k$ is a diagonal matrix defined as:

$$[Q]^k = \left(diag\left[\left([S]^k \right)^t . [S]^k \right] \right)^{1/2}; \qquad Q_{i,i} = \sqrt{\sum_{j=1}^{pt} S_{j,i}^2} , \quad i = 1,...,np .$$

The damping value λ is increased up to reach the condition where $F_{obj}^{k+1} < F_{obj}^{k}$. The iterative process goes on until reaching the convergence conditions of the parameters estimation process.

- The *FRFs* can be in linear scale (*FRF*) and logarithmic scale $(Log_{10}(FRF), 20*Log_{10}(FRF))$;
- There is an external penalty function (*w*: penalty coefficient) to the inequality constrains imposed to the parameters $(min \le p_i \le max)$:

$$F_{obj} = F_{obj} + w(max - p_i)^2 , \text{ se} : p_i > max; \; F_{obj} = F_{obj} + w(p_i - min)^2 , \text{ se} : p_i < min .$$

8. The Fitting Numerical Simulation

The system sketch in Fig. (5) represents the rotor-coupling-bearing model used to verify the fitting process of the coupling parameters in the mechanical system. Table (1) shows the dynamic and physical characteristics of several components of the mechanical system. The Finite Element Model developed in the simulation is illustrated in Fig. (6). The FEM considers each modelling criterion discussed previously. These models are used in the fitting process of the experimental FRFs (*FRD, FRF*).
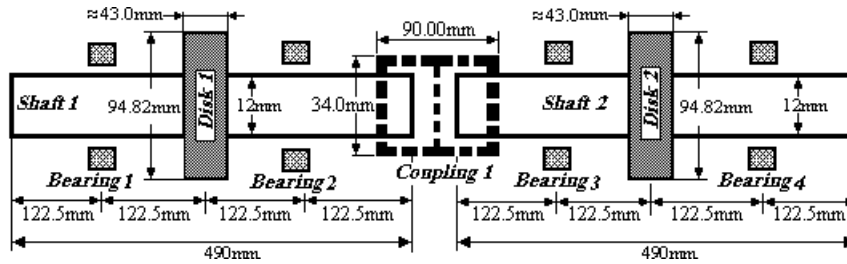

Figure 5. Sketch of simulated Rotor-Coupling-Bearing System.

Table 1. Dynamic and Physical Properties of the simulated mechanical system.

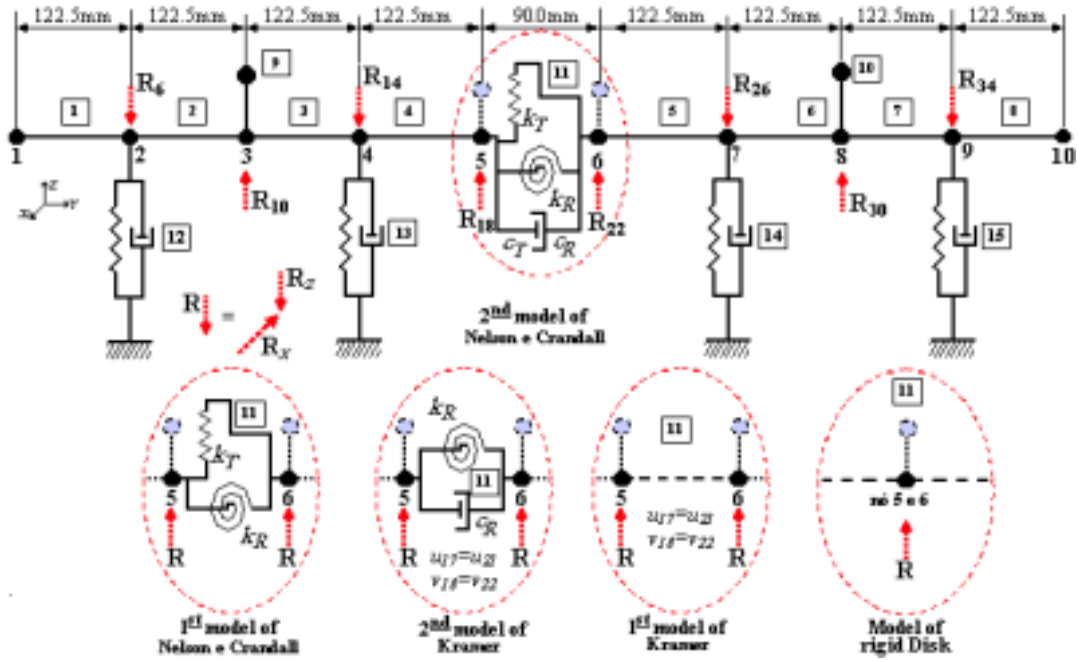|		
Shafts: Density = 7759.255kg/m^3 , Young Modulus = $1.936*10^{11}$N/m^2 , de Poisson coefficient = 0.3 Shear factor = 0.9 , Viscous damping factors: (qz_k = $22.989*10^{-6}$, qz_m = 15.691)		
Bearings 1	**Stiffness:** k_{xx}=$5.0*10^7$ N/m, k_{xz}=0.0 N/m, k_{zz}=$7.0*10^7$ N/m, k_{zx}=0.0 N/m **Damping:** c_{xx}=$5.0*10^2$ Ns/m, c_{xz}=0.0 Ns/m, c_{zz}=$7.0*10^2$Ns/m, c_{zx}=0.0 Ns/m	**Disk 1:** Density = 6303.235kg/m^3
2	**Stiffness:** k_{xx}=$7.0*10^7$ N/m, k_{xz}=0.0 N/m, k_{zz}=$9.0*10^7$ N/m, k_{zx}=0.0 N/m **Damping:** c_{xx}=$3.0*10^2$ Ns/m, c_{xz}=0.0 Ns/m, c_{zz}=$5.0*10^2$Ns/m, c_{zx}=0.0 Ns/m	
3	**Stiffness:** k_{xx}=$5.0*10^7$ N/m, k_{xz}=0.0 N/m, k_{zz}=$7.0*10^7$ N/m, k_{zx}=0.0 N/m **Damping:** c_{xx}=$5.0*10^2$ Ns/m, c_{xz}=0.0 Ns/m, c_{zz}=$7.0*10^2$Ns/m, c_{zx}=0.0 Ns/m	**Disk 2:** Density = 6303.235kg/m^3
4	**Stiffness:** k_{xx}=$7.0*10^7$ N/m, k_{xz}=0.0 N/m, k_{zz}=$9.0*10^7$ N/m, k_{zx}=0.0 N/m **Damping:** c_{xx}=$3.0*10^2$ Ns/m, c_{xz}=0.0 Ns/m, c_{zz}=$5.0*10^2$Ns/m, c_{zx}=0.0 Ns/m	
Coupling	Inner radius = 6.0mm , Outer radius = 17.0mm , Equivalent thickness = 43.115mm	
	Equivalent Density = 2758.219kg/m^3	
	Translational Stiffness = $46.095*10^3$ N/m; Translational Damping = 10.949 Ns/m	
	Rotational Stiffness = $22.076*10^1$ Nm/rad; Rotational Damping = $10.949*10^{-6}$ Nms/rad	

Figure 6. FEM to the Rotor-Coupling-Bearing System.

8.1. The Fitting of the Unbalance Response Function (*FRDs*)

The sensitivity analysis of the *FRDs* in the operational frequency range of the rotor, with respect to the coupling parameters in the 2nd Nelson and Crandall model, shows that the *FRDs* corresponding to the 9, 10, 17, 18 d.o.f. are the most sensitive to the majority of the coupling parameters, as in Fig. (7).
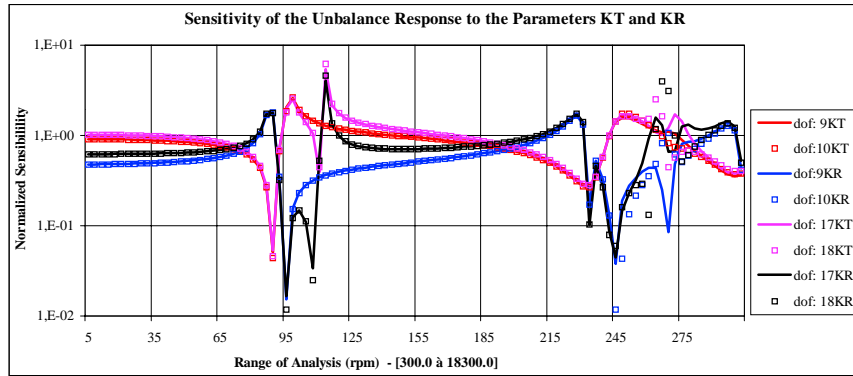

Figure 7. *FRDs* sensitivity of the simulated system to the stiffness parameters.

Once the most sensitive *FRDs* are defined, a simulation of the experimental *FRDs* is carried on (*FRDs_exp*), according with Eq. (19). In this equation, the noise is introduced by the formulation given by Dos Santos J., Ferraz F. (2001). Each point of the experimental *FRDs* is evaluated by:

$$ f_{e_i} = f_{s_s} + f_{s_s} * \frac{\beta_a}{100} * rand[-1,1] + \sqrt{\sum_{j=1}^{j=n} f_{s_j}^2 \Big/ n} * \frac{\beta_s}{100} * rand[-1,1]. \qquad (19) $$

Where: $rand$[-1,1] represents a random number between −1 and +1; f_{s_i} is the *i-th* component of the FEM simulated *FRD*; is the *i-th* component of the experimental *FRD*; n is the number of points of each *FRD*; β_a is the aleatory factor of the noise expression (10%); β_s is the systematic error of the noise expression (1%). The residual unbalance for each rigid disk is 15x10^{-5}kgm with a phase angle of 90[o] between them. The residual unbalance in disk 1 is located at 0[o] from *Z-axis* and the frequency range of analysis is 300 to 18300 rpm.

Once the experimental *FRDs* are evaluated from Eq. (19) for the four d.o.f. of the coupling, the fitting process to the model presented in Fig. (6) can be carried on. The fitting process uses the *FRDs* in the four d.o.f. simultaneously and the starting points of the parameters are approximately (1/10) times the values used to obtain the experimental

FRDs. The results of the fitting process are showed in Fig. (8) to d.o.f. 17 and 18. The results of this process are in Table (2).
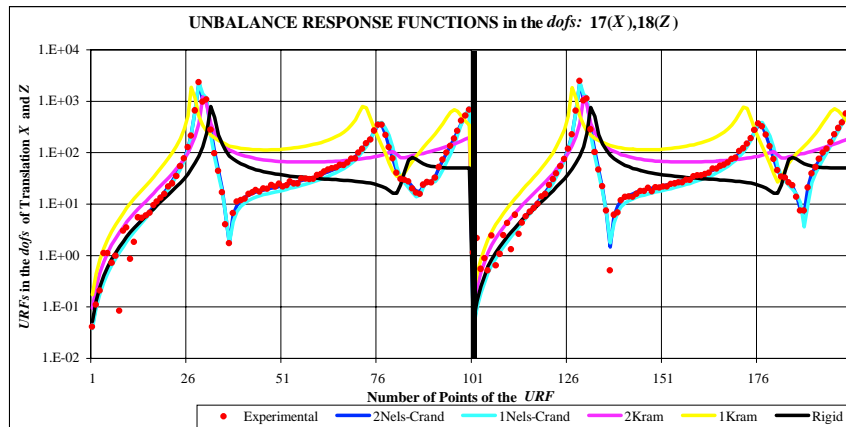

Figure 8. Fitting results of the simulated experimental *FRDs*.

Table 2. Estimation Process Data for the parameters of each Coupling Model Analysed.

Parameters	2nd Nelson - Crandall		1st Nelson - Crandall		2nd Kramer		1st Kramer	Rigid
Real Value	Adjusted	Error %	Adjusted	Error %	Adjusted	Error %		
k_T=46.095*10^{3}N/m	46.870*10^3	1.68	41.134*10^3	10.76	---	---	---	---
k_R=22.076*10^{1}Nm/rad	22.399*10^1	1.46	21.761*10^1	1.43	84.364*10^1	282.15	---	---
c_T=10.949Ns/m	10.922	0.25	---	---	---	---	---	---
c_R=10.949*10^{-6}Nms/rad	14.581*10^{-4}	∞	---	---	23.171*10^{-2}	∞	---	---
Error %		18.48		25.97		292.66	466.30	229.46
# Iterations		54		17		35	---	---
# Evaluated Functions		569		161		389	---	---

8.2. Fitting of the Frequency Response Functions

The sensitivity analysis of the *FRFs* (inertance), considering the 2nd Nelson and Crandall model, shows that the *FRFs* to the 22, 25, 30, 34 d.o.f. were the most sensitive with respect to the coupling parameters. The *FRFs* were obtained from an aleatory external force (Gauss Distribution) applied in the direction of 10 d.o.f. in the model. The range to the excitation force is 200 to 400Hz. The system rotational frequency is 10000rpm. Once the most sensitive *FRFs* are defined with respect to the coupling parameters, the simulated experimental *FRFs* (inertance) are also obtained, with the 2nd Nelson and Crandall model. Afterwards, the fitting process can be carried on, considering all the experimental *FRFs* simultaneously in the four d.o.f. of the coupling. The process results, for all coupling models proposed, are presented in Fig. (9) to 22 and 25 d.o.f. Table (3) shows the results of the fitting process.
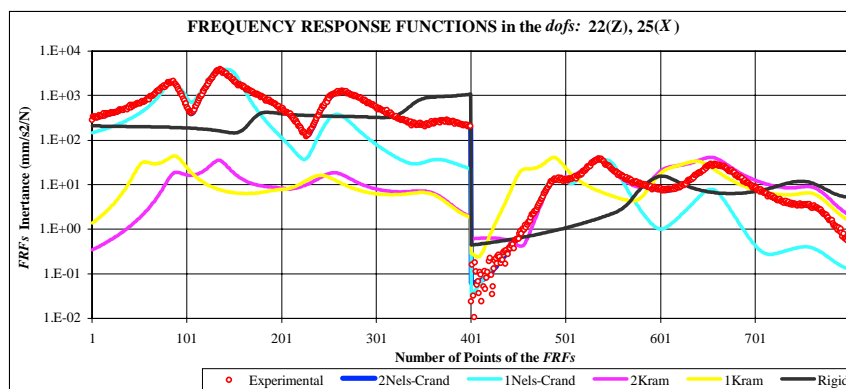

Figure 9. Fitting Results to the *FRFs* (inertance) of the system.

Table 3. Estimation Process Data for the parameters of each Coupling Model Analysed by using the *FRFs*.

Parameters	2nd Nelson e Crandall		1st Nelson e Crandall		2nd Kramer		1st Kramer	Rigid
Real Value	Adjusted	Error %	Adjusted	Error %	Adjusted	Error %		
k_T=46.095*10^{3}N/m	45.866*10^3	0.50	27.354*10^3	40.66	---	---	---	---
k_R=22.076*10^{1}Nm/rad	22.062*10^1	0.06	19.590*10^1	11.26	21.599*10^1	2.16	---	---
c_T=10.949Ns/m	10.971	0.20	---	---	---	---	---	---
c_R=10.949*10^{-6}Nms/rad	50.723*10^{-7}	53.68	---	---	99.755*10^{-8}	90.89	---	---
Error %		6.377		61.427		125.988	180.749	166.965
# Iterations		16		66		9	---	---
# Evaluated Functions		202		607		220	---	---

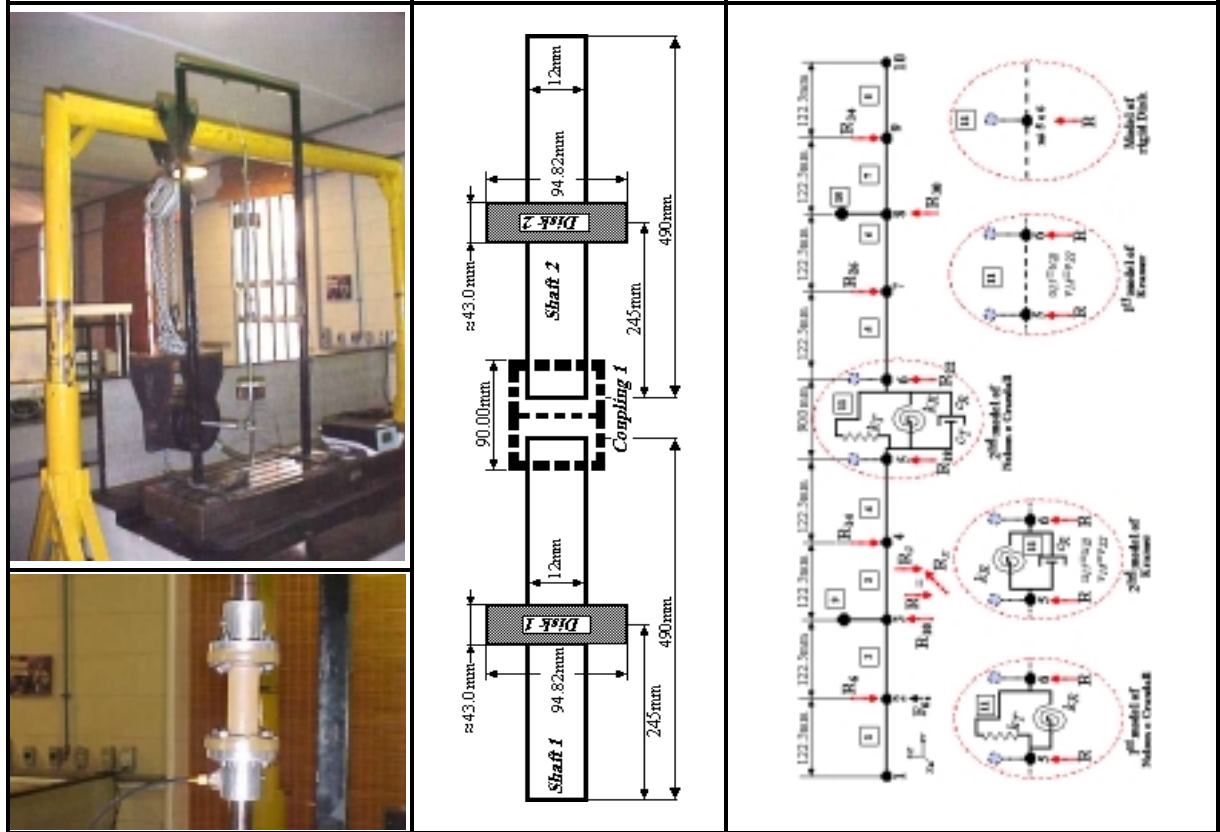## 9. Fitting of the Experimental Test Data

Figure 10. Experimental set up – Sketch of the System – Modal Analysis Free-Free Model of the Rotor-Coupling System.

The modal analysis was accomplished in the system shown in Fig. (10), free-free condition, to obtain the *FRFs* (inertance) in the 6, 10, 14, 18, 22, 26, 30, 34 d.o.f. The random external force (Gauss Distribution) is applied on the 6 d.o.f. using an electromagnetic exciter in a frequency range of 0 to 500Hz. The analysis was carried on in the range of 0 to 250Hz. The sensitivity analysis considered the *FRFs* from the FEM in Fig. (10) with respect to the coupling parameters in the 2nd Nelson and Crandall model. The objective is to represent the flexible coupling made of Neoprene. The results show that the *FRFs* (inertance) in the 6, 10, 14, 18, 22, 30 d.o.f. are the most sensitive in the process. Fig. (11) shows the sensitivity of the *FRFs* in the 14, 18, 22 d.o.f.. The experimental *FRFs* at the 14, 18, 22 d.o.f. are simultaneously used in the fitting process of the couplings models in the rotating system showed in Fig. (10). The results obtained from the fitting process are presented in Fig. (12). Notice that only two d.o.f. (18 and 22) are plotted in this graphic. Table (4) gives the data of the estimation process for the parameters of each coupling model using the experimental *FRF* .
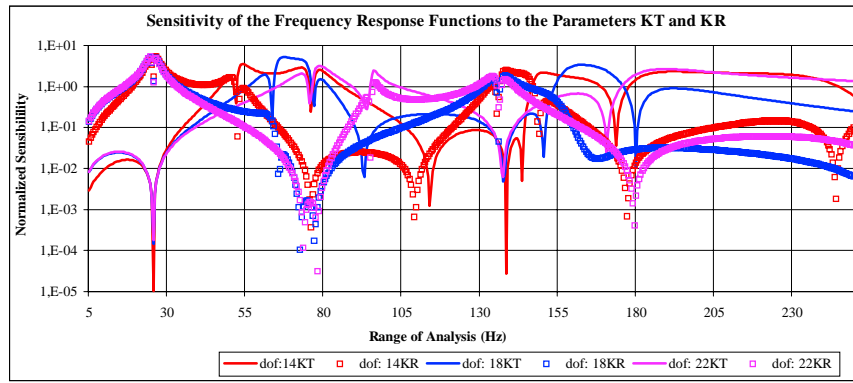
Figure 11. *FRFs* Sensitivity to the 2nd Nelson and Crandall Model – Rotor-Coupling System.
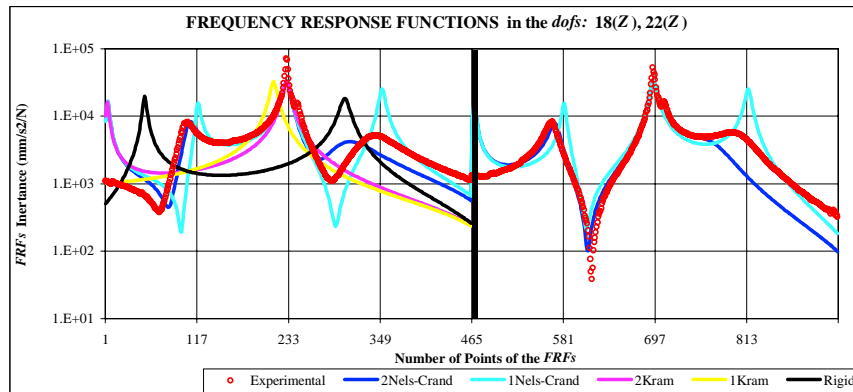

Figure 12. Fitting Results to the experimental *FRFs* (inertance) of the system in Figure 10.

Table 4. Estimation Process Data for the parameters of each Coupling Model by using the experimental *FRFs*.

Parameters	2nd Nelson - Crandall	1st Nelson - Crandall	2nd Kramer	1st Kramer	Rigid
	Adjusted	Adjusted	Adjusted		
k_T : N/m	$43.609*10^3$	$65.659*10^3$	---	---	---
k_R : Nm/rad	$21.890*10^1$	$21.949*10^1$	$21.173*10^1$	---	---
c_T : Ns/m	11.511	---	---	---	---
c_R : Nms/rad	$42.965*10^{-7}$	---	$61.924*10^{-6}$	---	---
Error %	77.627	92.123	118.328	68.183	320.89
# Iterations	70	92	97	---	---
# Evaluated Functions	787	835	935	---	---

10. Conclusions

An estimation method was implemented to fit parameters of coupling simplified models in Rotor-Coupling-Bearing System. The *FRFs* (unbalance response or transfer functions) are used for this purpose. The fitting procedure applies the Non-linear Minimum Square Method. In the sensitivity analysis for the 2nd Nelson and Crandall model, using the *FRDs* and the *FRFs* (inertance), different d.o.f. were more or less sensitive with respect to the coupling parameters. This can be explained by the mode shape of the rotor, which can make some d.o.f. more significant than the others in a fitting process. In the model fitting using the experimental *FRFs* generated by simulation (2nd Nelson and Crandall model with a noise effect), the convergence of the coupling parameters leaded to the expected parameters supposed to be real. This fact is true to the different models analysed, for the parameters which present the highest sensitivity in the frequency range of analysis. In these cases, the maximum value of the error was 1.7% for the 2nd Nelson and Crandall model. It is important to stand out that the 2nd Nelson and Crandall model takes into account stiffness and damping parameters to the coupling. Figs. (8), (9) and (12) show that the models with the best fitting consider at least stiffness parameters to the coupling. The rigid models can not reproduce the *FRFs*. Finally, the fitting process was applied to the experimental *FRFs* (inertance) described in Fig.10 (Free-Free Modal Analysis of the Rotor-Coupling System). In this case, the model with the best fitness of the experimental *FRFs* is the 2nd Nelson and Crandall model, followed by those models which consider stiffness and/or damping coefficients for the coupling. However, the rigid models are not able to fit any experimental *FRFs* as well. The fitting process quality can change also with the range of analysis. This fact is due to the

non-linear characteristics of the coupling, which can be more significant in high rotational speed. In this case, the linear models proposed here are not adequate to represent the dynamical behaviour of the coupling.

11. Acknowledgements

12. References

Kramer, E., 1993, "Dynamics of Rotors and Foundations", New York, Springer-Verlag. pp. 381.

Nelson, H. D., Crandall, S. H., 1992, "Analytic Prediction of Rotordynamic Response". In: EHRICH, F. F., Handbook of Rotordynamics. United States of America, McGraw-Hill, Inc., Cap.2, pp. 2.1-2.84.

Sekhar, A. S., Rao, A. S., 1996, "Vibration analysis of Rotor–Coupling–Bearing System with Misaligned Shafts". International Gas Turbine and Aeroengine Congress & Exhibition.

Xu, M., Marangoni, R. D., 1994, "Vibration Analysis of a Motor-Flexible Coupling-Rotor System Subject to Misalignment and Unbalance", Part I: Theoretical model and analysis, Part II: Experimental validation. Journal of Sound and Vibration, Vol. 176, pp. 663-691.

Arruda, J. R. F., 1987, "Rotor finite element model adjusting". In: *Proceedings of the 9th Brazilian Congress of Mechanical Engineering*, Florianópolis, SC, pp.741-744.

Arruda, J. R. F., 1989, "Rotor model adjusting by unbalance response curve-fitting". In: *Proceedings of the 7th International Modal Analysis Conference,* v.1, Society for Experimental Mechanics, pp.479-484.

Duarte, M. V., 1994, "Ajuste de modelos dinâmicos de estruturas com não linearidades concentradas". Campinas: Faculdade de Engenharia Mecânica, Universidade Estadual de Campinas, 190p., Tese (Doutorado).

Dos Santos, J.M.C., Ferraz, F.G., 2001, "Block-Krylov Component Synthesis and Minimum Rank Perturbation Theory for Damage Detection in Complex Structures". In: *Proceedings of the IX DINAME*, Florianópolis-SC-Brazil, pp.329-334.

Tapia, A. T., Cavalca, K. L., 2001, "Efeito da Modelagem dos Acoplamentos Flexíveis nos Sistemas Mecânicos". XVI Congresso Brasileiro de Engenharia Mecânica, Uberlândia – MG – Brasil, Vol. 10, pp. 44-53.

Tapia, A. T., Cavalca, K. L., 2002, "Modelling effect of flexible and rigid couplings in mechanical systems", Proceedings of the Sixth International Conference on Rotor Dynamics, Vol. 1, Sydney, Australia, pp. 420-429.

Tapia, A. T., 2003, "Modelagem dos Acoplamentos Mecânicos nos Sistemas Horizontais Rotor-Acoplamento-Mancal". Campinas: Faculdade de Engenharia Mecânica, Universidade Estadual de Campinas, 250p. Tese (Doutorado).